Subpopulation-Resolved Photon Statistics of Single-Molecule Energy Transfer Dynamics

Daniel Nettels and Benjamin Schuler

(Invited Paper)

***Abstract*—We present a technique that combines the power of single-molecule spectroscopy to separate subpopulations in a heterogeneous ensemble with submicrosecond correlation spectroscopy based on a Hanbury Brown and Twiss detection scheme. The use of four detectors allows such measurements to be performed with the spectral separation necessary for Förster resonance energy transfer (FRET), which has become an important tool to study biomolecular structure and dynamics in single-molecule experiments. Our approach avoids the common limitations caused by the dead times of detectors and counting electronics in conventional single-molecule FRET experiments, and thus, allows access to dynamics down to the picosecond range. We illustrate the technical aspects of the method with recent measurements of the rapid chain dynamics in the unfolded state of a small protein.**

***Index Terms*—Fluorescence correlation spectroscopy, Förster resonance energy transfer (FRET), protein folding, single-molecule spectroscopy.**

I. Introduction

In recent years, single-molecule fluorescence spectroscopy has become a powerful tool for studying a wide range of molecular systems, especially biomolecules [1]–[3]. In particular, the measurement of Förster resonance energy transfer (FRET) [4], [5] between two (or more) fluorophores attached to different positions in the molecule plays an increasingly prominent role [6]–[10]. FRET allows the measurement of inter- and intramolecular distances in the range of 1–10 nm. One of the most powerful aspects of single-molecule FRET has been the possibility to investigate the properties of subpopulations even in heterogeneous mixtures of molecules [11] both under equilibrium and nonequilibrium conditions, where an ensemble experiment would only yield a transfer efficiency averaged over the entire population. The most notable examples include measurements on nucleic acids and proteins, the most versatile biological macromolecules.

The molecular distance information accessible through FRET experiments is frequently complemented using fluorescence correlation spectroscopy, which provides information about fluctuations in molecular systems. For molecules freely diffusing in solution, dynamic processes that can be observed range from the photophysics of the fluorophores to the intramolecular distance fluctuations and translational diffusion [12]. However, timescales in the submicrosecond range are difficult to access due to limitations of detectors and counting electronics. The avalanche photodiodes typically used for single-molecule fluorescence detection exhibit dead times in the range of 100 ns following the detection of a photon. Similarly, many counting cards have dead times of up to a few hundred nanoseconds. As a consequence, dynamics on these time scales and below are not accessible. A possibility to avoid these limitations and to access photon statistics in the nanosecond range and below is to use a Hanbury Brown and Twiss detection scheme [13]–[20]. In this case, two detectors are used, one acting as a start and the other as a stop channel. The photons are distributed statistically between them using a 50/50 beam splitter, and are used to determine interphoton intervals, from which the intensity correlation function can be determined. However, this type of experiment does not intrinsically provide the separation of subpopulations in an ensemble required for the investigation of heterogeneous samples.

Here, we present a method that combines both techniques, and enables subpopulation separation by single-molecule spectroscopy and fast correlation spectroscopy using a Hanbury Brown and Twiss configuration. Four detectors are used to enable the spectral separation necessary for FRET, and correlation functions are obtained from individual subpopulations by first sorting the single molecules diffusing through the confocal observation volume according to their transfer efficiencies. We recently used this approach for probing the dynamics in the unfolded state of a small protein (Csp) under conditions where only part of the population is unfolded [21]. The proteins were labeled terminally with green fluorescent donor and red fluorescent acceptor dyes for FRET, and were observed with a confocal microscope while freely diffusing in buffer solution. Our method enabled us to measure the rapid fluctuations of the end-to-end distance in the unfolded polypeptide chain in the nanosecond range, independent of the signal originating from the subpopulation of folded protein molecules present in the solution at the same time. Here, we describe this method in technical detail. It should be valuable for a wide range of heterogeneous systems, where both distance information and rapid dynamics are of interest.

II. Separation of Subpopulations Using Single-Molecule FRET Spectroscopy

The basic principle of FRET is illustrated in Fig. 1(a). One of the two dyes, the donor, is excited by means of resonant laser light. The donor then either decays to its ground state and emits a fluorescence photon (rate constant k_D), or its excitation energy is transferred to the other dye, the acceptor, by means of

Manuscript received January 14, 2007; revised June 14, 2007. This work has been supported by the Human Frontier Science Program and the Swiss National Science Foundation.

The authors are with the Department of Biochemistry, University of Zurich, 8057 Zurich, Switzerland (e-mail: nettles@bioc.uzh.ch; schuler@bioc.uzh.ch).

Digital Object Identifier 10.1109/JSTQE.2007.902848

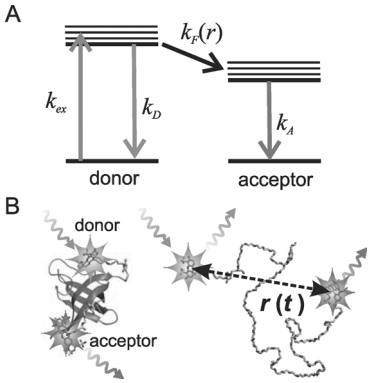

Fig. 1. Basic principle of FRET. (a) Donor and acceptor level scheme of a FRET-coupled dye pair. The donor is excited by resonant laser light (rate constant k_{ex}). It either decays back to the ground state directly, and a donor photon is emitted, or the excitation energy is transferred to the acceptor with the distance-dependent rate constant $k_F(r)$, and an acceptor photon is emitted (rate constant k_A). (b) Protein (Csp) is terminally labeled with donor and acceptor chromophores. In its folded conformation (left side), the dyes are in close proximity, and high energy transfer is observed. When the protein is unfolded (right side), the inter-dye distance is greater on average than in the folded state, resulting in a lower average transfer efficiency. The instantaneous transfer efficiency, however, fluctuates ($r(t)$) on the same time scale as the end-to-end distance of the polypeptide chain.

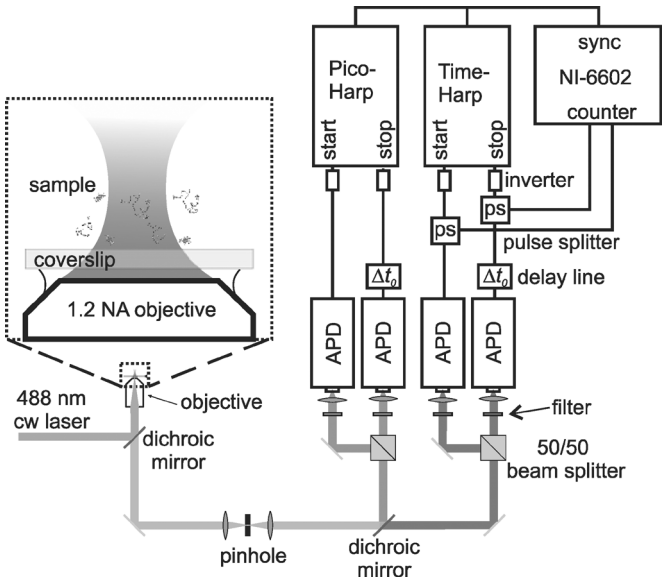

Fig. 2. Schematic of the instrument used for confocal single-molecule detection and recording of interphoton time correlation functions (see text for details).

FRET (rate constant k_F). In the latter case, the acceptor becomes excited, and acceptor fluorescence is observed as the acceptor returns to its ground state by spontaneous decay (rate constant k_A). According to Förster's theory [4], the dependence of the transfer rate k_F on the inter-dye distance r can be expressed as $k_F(r) = k_D(R_0/r)^6$. (Here, we assume complete orientational averaging of the dye transition dipoles during the donor-excited state lifetime.) R_0, the Förster radius of the dye pair, is typically in the range of a few nanometers.

In the single-molecule FRET experiments (see Fig. 2), the dye-labeled Csp protein molecules diffuse freely in the solution. Occasionally, a protein diffuses through the laser focus of the confocal microscope, and the emission of a burst of donor and acceptor photons is recorded by single-photon detectors. The transfer efficiency defined as $E \equiv k_F/(k_F + k_D) = 1/[1 - (r/R_0)^6]$ can be determined for each burst as

$$E = n_A/(n_A + n_D) \tag{1}$$

from the number n_D and n_A of the measured donor and acceptor burst photons, respectively (n_D and n_A are assumed to be background-subtracted, corrected for different quantum yields of the fluorophores and for crosstalk and the different efficiencies of the detection channels). It is to be noted that the values obtained for E are time-averaged over all transfer efficiency changes that occur during the passage through the confocal volume, e.g., rapid distance changes in the unfolded state. Fig. 3(a) shows a transfer efficiency histogram obtained from photon bursts measured at a concentration of 50 pM Csp in a buffer solution containing 1.5 M of the denaturant guanidinium chloride (GdmCl). Three subpopulations are resolved: folded protein molecules with a transfer efficiency E close to 1, unfolded molecules with $E \approx 0.5$, and molecules lacking an active acceptor chromophore with $E \approx 0$ [22], [23]. The separation of subpopulations is not perfect, as can be seen from the empirical distribution functions fit to the three peaks [solid lines in Fig. 3(a)]. However, the assignment of a protein to one of the

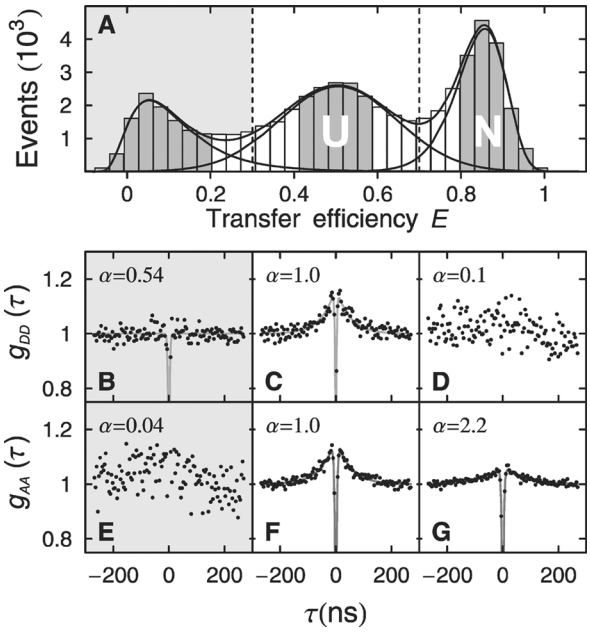

Fig. 3. Intensity autocorrelation functions of the subpopulations identified in single-molecule experiments. (a) Transfer efficiency histogram at 1.4 M GdmCl fit with three peaks (black lines) corresponding to the folded or native ("N", high E) and unfolded ("U", $E \approx 0.5$) subpopulations, and molecules lacking an active acceptor ($E \approx 0$, background shaded in grey). The ranges of E used for extracting the specific normalized donor and acceptor autocorrelation functions (b)–(d) g_{DD} and (e)–(g) g_{AA} are shaded. Fits to g_{DD} and g_{AA} are shown. The normalized signal amplitude α for each correlation function is given relative to the unfolded state ($\alpha = 1$). g_{DD} and g_{AA} were calculated from the corresponding interphoton time distributions by using (2) and by correcting triplet state components (see text for details). Figure is taken from [21].

subpopulations is reliable if the measured transfer efficiency is restricted to one of the E ranges of the histogram shaded.

The central idea of our method is to generate interphoton time histograms for each separated subpopulation using the detection times of the photons that belong to the corresponding photon bursts. In the limit of short interphoton times (compared to the mean interphoton time during a burst), these histograms are essentially equivalent to fluorescence correlation functions and, thus, provide direct information on the rapid FRET dynamics of the dye pairs. For measuring interphoton times shorter than the dead times of the photon detectors, it is necessary to employ a Hanbury Brown and Twiss detection scheme. Here, the photons are randomly distributed between two detectors, which are connected to the start and stop input channels of a photon counter. The time intervals between successive photons detected at the start and the stop channel, respectively, are measured. The results of our subpopulation-resolved FRET dynamics measurements are presented in Fig. 3(b)–(g) as donor and acceptor fluorescence autocorrelation functions. They will be discussed following a detailed description of the instrument.

III. Instrumentation and Materials

A. Protein Synthesis and Labeling

Csp with Cys residues at positions 2 and 67 were expressed recombinantly, purified and labeled as described previously [22], [24]. In order to exclude potential complications due to proline cis-trans isomerization in Csp, Pro57 had been replaced with Gly. Dye labeling was carried out by procedures described by the manufacturer (Invitrogen). Alexa Fluor 488 maleimide was reacted with the protein, and singly labeled protein was separated from unlabeled and doubly labeled protein by ion exchange chromatography (Mono Q HR 5/5, GE Healthcare). The fractions containing singly labeled Csp, as confirmed by electrospray ionization mass spectroscopy, were labeled with Alexa Fluor 594 maleimide. Doubly labeled protein was again separated from singly labeled protein by ion exchange chromatography. All the experiments were performed in aqueous buffer solutions containing 50-mM sodium phosphate, 0.001% Tween 20 (to minimize surface adhesion), the concentration of GdmCl given with the respective measurement, and were adjusted individually to pH 7.

B. Confocal Microscope

Single-molecule fluorescence was observed using a MicroTime 200 confocal microscope (PicoQuant, Berlin, Germany) equipped with a CW solid-state diode-pumped laser (Coherent Sapphire 488-200) operating at 488 nm (average radiant power at the sample: 100 μW), a 1.2 NA, 60$\times$ microscope objective (Olympus UplanApo 60$\times$/1.20 W), and a 100 μm confocal pinhole (see Fig. 2). A dichroic mirror (Chroma 585DCXR) separated the donor and acceptor fluorescence. Subsequently, each fluorescence component was divided randomly by a 50/50 beam splitter between a pair of two avalanche photodiodes (APDs, PerkinElmer Optoelectronics SPCM-AQR-15). Additional interference filters (Chroma HQ525/50 and Omega 525AF45, respectively, for the donor APDs, Chroma 600HQLP and HQ640/100, respectively, for the acceptor APDs) completed spectral separation of the sample fluorescence and served to suppress the mutual detection of APD breakdown flashes in the infrared [25].

C. Photon Counting Electronics and Data Acquisition

Each of the two APD pairs was connected to a time-correlated single-photon counter: the donor detectors to a PicoHarp 300 and the acceptor detectors to a TimeHarp 200 (both PicoQuant). We denote the two input channels of each card as start and stop channels. To avoid crosstalk between the two channels at short time intervals and to simplify data analysis (see below), electronic time delays Δt_0 are imposed onto the stop channels. Attenuating signal inverters were included to meet the input signal specifications of the photon counters. Where needed, the transmission lines were terminated with 50-Ω resistors to avoid signal reflections.

The PicoHarp 300 is a stand-alone device with a USB connection to a PC [28]. Here, we used the time-tagged 'T2' mode, where the two input channels record the incoming photon arrival times independently with a 4-ps time resolution. The arrival times are stored in a FIFO memory buffer before they are read out via the USB interface. In our experiment, the PicoHarp 300 recorded the donor photon data. A custom-developed software (written in C++) scans the incoming photon stream for start–stop photon pairs with an interphoton time Δt less than a maximum value $\Delta t_{\max}$, up to which the interphoton time histograms will be generated. The arrival times of these photons are stored in the hard disk. Simultaneously, donor photon counts from both detectors were combined in 1-ms bins and stored in hard disk as well. These data will serve to identify the photon bursts originating from individual molecules. It is to be noted that without data reduction, i.e., if the arrival time of every single photon was stored in the hard disk, measurements of 50 h (the integration time necessary for obtaining the data in Fig. 3) would result in data file sizes of more than 10 GB, which are still impractical to process.

The TimeHarp 200 is a PCI-card housed in a PC. Its two input channels cannot count photons independently as in the case of the PicoHarp 300, but they are restricted to measuring the start–stop photon pairs. Upon receipt of a start pulse in the start channel, the time Δt is measured until a photon is detected at the stop channel. We chose to measure Δt with a time resolution of 304 ps, resulting in a maximum interphoton time of $\Delta t_{\max} = 1.2\,\mu$s (the TimeHarp 200 provides 4096 time bins for time-correlated single-photon photon counting). If no photon is detected at the stop channel during this time interval, then the card restarts to wait for a start photon. We operated the card in its "TTTR" mode: The Δt values are stored together with the time t of the corresponding start–stop event on hard disk; t is stored with a 100-ns resolution. In our experiments, the TimeHarp 200 recorded the acceptor photon data.

Since the TimeHarp 200 records only start–stop photon pairs with $\Delta t < \Delta t_{\max}$ and discards all other photons, we employed, in addition, two counting channels of an NI-6602 PCI card

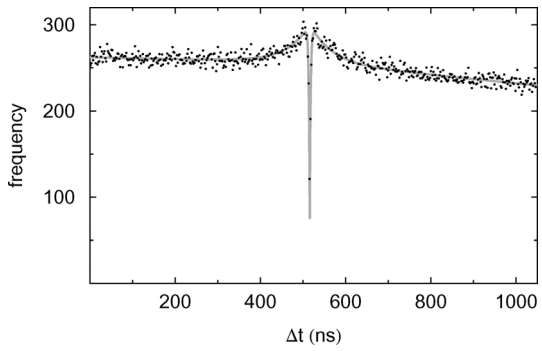

Fig. 4. Donor interphoton time histogram obtained from the bursts with E in the range between 0.4 and 0.6, i.e., from unfolded protein molecules. The experimental data were fit with (2) and (3).

(National Instruments) for combining the acceptor photon counts in 1-ms bins. Furthermore, the NI-6602 served to synchronize the measurements of all three cards. For this purpose, one of its digital input/output (I/O) channels (labeled as "sync" in Fig. 2) generated TTL pulses with 1-s time separation, which were sent to PicoHarp 300 and the TimeHarp 200. For synchronization purposes, both single-photon counting cards were equipped with input channels to record time markers. For each synchronization signal received, a marker record containing the reception time of the pulse is generated. The marker records are used during data acquisition to synchronize the 1-ms binning of donor and acceptor photons. For the later synchronization of the start–stop events, with the binning data, the marker records were also saved on the hard disk.

IV. Measurements

The acquisition time of the data shown in Fig. 3 was 50 h. The sample solution was replaced every 10 h to avoid sample deterioration. After subtracting the background signal from the millisecond-binned fluorescence data, sequences of adjacent bins with at least 40 donor or acceptor photons and a combined total of at least $n_A + n_D = 80$ photons were identified as significant bursts. To account for the different quantum yields of the fluorophores and the different efficiencies of donor and acceptor photon detection, the donor counts per bin were multiplied by the correction factor $\gamma = 1.25$ prior to burst identification (γ was estimated using a sample of known transfer efficiency [23]). An energy transfer efficiency E was assigned to each identified burst using (1). Transfer efficiency histograms as shown in Fig. 3(a) were generated from the E values of all identified bursts.

Finally, we reduced the start–stop data by keeping only those interphoton intervals that coincide with bursts within a given range of E in the transfer efficiency histogram [one of the E regions shaded in Fig. 3(a)]. From the Δt values of the respective subsets, subpopulation-specific interphoton time distributions were calculated. Fig. 4 shows the donor interphoton time histogram obtained from the bursts with E in the range between 0.4 and 0.6, i.e., from unfolded protein molecules. The distribution has a sharp minimum at about 500 ns, corresponding to the time delay Δt_0 imposed onto the stop channel of the donor photon counter. The relation between the interphoton time distributions $\phi_{i,i}(\Delta t)$ and the autocorrelation functions $g_{\mathrm{ii}}(\tau)$ with $i = D, A$, can to a good approximation, be expressed as

$$\phi_{ii}(\Delta t) = Ae^{-\Delta t/t_i} g_{ii}(\Delta t - \Delta t_0). \tag{2}$$

where A is an overall amplitude, and t_i^{-1} is the mean photon rate detected by the APDs during a photon burst. The exponential decay term describes the decreasing probability for the occurrence of longer interphoton times. Apart from this slight overall exponential decrease (visible at low and high values of Δt, Fig. 4), the interphoton distribution is equivalent to the autocorrelation function $g_{ii}(\tau)$, which is by definition the conditional probability that a photon is detected at time τ after the emission of a photon was observed. This probability is normalized by the probability to detect a photon at an arbitrary time. Hence, in the limit of long lag times τ, the correlation function is one, because then, the two events of detecting the photons become statistically independent.

V. Results and Discussion

The $g_{DD}(\tau)$ contained in the data of Fig. 4 exhibits a drop in amplitude at $\tau = 0$. This photon antibunching is characteristic of individual quantum systems that cannot emit two photons simultaneously; it decays on the time scale of the fluorescence lifetime of the dyes [14], i.e., within a few nanoseconds. More interestingly, pronounced photon bunching—an additional component in $g_{DD}(\tau)$ with positive amplitude—is observed in the 50-ns range. We attribute this photon bunching to the end-to-end distance dynamics of the unfolded state: if a donor photon is emitted at $t = 0$, the chain ends are likely to be far apart at that instant, corresponding to a low rate of energy transfer $k_F(r)$. A very short time later, the ends will still be far apart, and the likelihood of emitting another donor photon will still be increased. However, at times much greater than the reconfiguration time of the chain, the molecule will have lost the "memory" of its initial configuration at $t = 0$, and the probability of donor emission will be determined by the average transfer efficiency. In other words, we expect an increased autocorrelation around $t = 0$ that decays approximately on the time scale of chain reconfiguration.

For a quantitative analysis of the subpopulation-resolved interphoton time distributions, we fit (2) to the data with

$$g_{ii}(\tau) = g_{AB}(\tau) g_B(\tau) g_T(\tau) = (1 - c_{AB}\, e^{-|\tau|/\tau_{AB}}) \times (1 + c_B\, e^{-|\tau|/\tau_B})(1 + c_T\, e^{-|\tau|/\tau_T}). \tag{3}$$

The first two factors in (3), $g_{AB}(\tau)$ and $g_B(\tau)$, describe the photon antibunching component and the bunching component due to FRET dynamics, respectively. An additional slower component with a relaxation time of $\tau_T \approx 3\ \mu$s was observed in all data sets, as expected from the triplet state lifetimes of the chromophores [26]. This component is accounted for by the third factor $g_T(\tau)$. We determined the triplet-state correlation time τ_T from independent conventional fluorescence correlation spectroscopy (FCS) measurements. All other parameters in (2) and (3) were fit to each of the six interphoton time distributions obtained from the donor and acceptor photons for each of the three subpopulations indicated in Fig. 3(a). Subsequently, we divided the data by $Ae^{-\Delta t/t_i} g_T(\Delta t - \Delta t_0)$ for obtaining the

correlation histograms corrected for triplet state dynamics as shown in Figs. 3(b)–(g). The values of α in Fig. 3 were calculated as $\alpha = A(1 + c_T)$ and normalized to 1 for the unfolded subpopulations. It is to be noted that the decay of the correlation function caused by translational diffusion of the molecules through the confocal volume was neglected in this analysis, because the corresponding millisecond time scale is outside the range of interest here.

Figs. 3(b) and (e) display the donor and acceptor autocorrelation histograms of the protein subpopulation lacking an active acceptor. $g_{DD}(\tau)$ lacks a bunching component as expected in the absence of FRET dynamics. Almost no photons were detected on the acceptor channels for this population. The resulting correlation histogram is correspondingly noisy and makes virtually no contribution to the overall signal. In contrast, for the unfolded subpopulation, both autocorrelation functions are well resolved, showing a bunching component with very similar time constants (donor $\tau_B = 49.2$ ns, acceptor $\tau_B = 51.6$ ns). Under identical conditions, this signal is absent in stiff polyproline peptides and protein labeled only with a donor chromophore [21], confirming that the bunching component in Fig. 3(c) and (f) is indeed due to the chain dynamics of the unfolded protein. The acceptor autocorrelation function $g_{AA}(\tau)$ of the folded subpopulation also shows a weak bunching component [Fig. 3(d)]. This might be due to the imperfect separation of subpopulations [Fig. 3(a)], but the slower relaxation compared to the unfolded state ($\tau_B = 67.2$ ns) could indicate an additional contribution from interactions of the chromophores with their specific environment in the folded state [21].

In summary, we have developed a method to measure the rapid distance dynamics of specific subpopulations present in an inhomogeneous ensemble of molecules via fluctuations in the transfer efficiency between two chromophores. The approach of combining the capability of single-molecule spectroscopy to separate subpopulations with the high time resolution of a Hanbury Brown and Twiss detection scheme should be applicable to a broad range of molecular systems, and will gain increasing popularity with the availability of latest generation counting cards [27], [28].

ACKNOWLEDGMENT

The authors would like to thank I. Gopich for helpful discussion on photon statistics and PicoQuant for technical help in the initial stages of the project.

REFERENCES

[1] W. E. Moerner, "A dozen years of single-molecule spectroscopy in physics, chemistry, and biophysics," *J. Phys. Chem. B*, vol. 106, no. 5, pp. 910–927, Feb. 7, 2002.

[2] X. S. Xie and J. K. Trautman, "Optical studies of single molecules at room temperature," *Annu. Rev. Phys. Chem.*, vol. 49, pp. 441–480, 1998.

[3] S. Weiss, "Fluorescence spectroscopy of single biomolecules," *Science*, vol. 283, no. 5408, pp. 1676–83, 1999.

[4] T. Förster, "Zwischenmolekulare Energiewanderung und Fluoreszenz," *Ann. Phys.*, vol. 6, no. 2, pp. 55–75, 1948.

[5] B. W. Van, Der Meer, G. I. Coker, and S. Y. S. Chen, *Resonance Energy Transfer: Theory and Data.* New York, Weinheim, Cambridge: VCH, 1994.

[6] T. Ha, T. Enderle, D. F. Ogletree, D. S. Chemla, P. R. Selvin, and S. Weiss, "Probing the interaction between two single molecules: Fluorescence resonance energy transfer between a single donor and a single acceptor," *Proc. Natl. Acad. Sci. USA*, vol. 93, no. 13, pp. 6264–6268, 1996.

[7] X. Zhuang and M. Rief, "Single-molecule folding," *Curr. Opin. Struct. Biol.*, vol. 13, no. 1, pp. 88–97, 2003.

[8] G. Haran, "Single-molecule fluorescence spectroscopy of biomolecular folding," *J. Phys.-Condens. Matter*, vol. 15, no. 32, pp. R1291–R1317, 2003.

[9] B. Schuler, "Single-molecule fluorescence spectroscopy of protein folding," *Chemphyschem*, vol. 6, no. 7, pp. 1206–1220, 2005.

[10] X. Michalet, S. Weiss, and M. Jäger, "Single-molecule fluorescence studies of protein folding and conformational dynamics," *Chem. Rev.*, vol. 106, no. 5, pp. 1785–1813, 2006.

[11] C. Eggeling, S. Berger, L. Brand, J. R. Fries, J. Schaffer, A. Volkmer, and C. A. Seidel, "Data registration and selective single-molecule analysis using multi-parameter fluorescence detection," *J. Biotechnol.*, vol. 86, no. 3, pp. 163–180, Apr. 2001.

[12] E. S. Elson and R. Rigler, in *Fluorescence Correlation Spectroscopy*, E. S. Elson and R. Rigler, Eds. Berlin, Germany: Springer-Verlag, 2001.

[13] R. Hanbury Brown and R. Q. Twiss, "Correlation between photons in two coherent beams of light," *Nature*, vol. 177, no. 4497, pp. 27–29, 1956.

[14] M. Ehrenberg and R. Rigler, "Rotational Brownian-motion and fluorescence intensity fluctuations," *Chem. Phys.*, vol. 4, no. 3, pp. 390–401, 1974.

[15] L. Fleury, J.-M. Segura, G. Zumofen, B. Hecht, and U. Wild, "Nonclassical photon statistics in single-molecule fluorescence at room temperature," *Phys. Rev. Lett.*, vol. 84, no. 6, pp. 1148–1151, Feb. 2000.

[16] P. Tinnefeld, C. Müller, and M. Sauer, "Time-varying photon probability distribution of individual molecules at room temperature," *Chem. Phys. Lett.*, vol. 345, pp. 252–258, 2001.

[17] A. J. Berglund, A. C. Doherty, and H. Mabuchi, "Photon statistics and dynamics of fluorescence resonance energy transfer," *Phys. Rev. Lett.*, vol. 89, no. 6, pp. 068101-01–068101-04, Aug. 2002.

[18] K. Weston, M. Dyck, P. Tinnefeld, C. Muüller, D. Herten, and M. Sauer, "Measuring the number of independent emitters in single-molecule fluorescence images and trajectories using coincident photons," *Anal. Chem.*, vol. 74, no. 20, pp. 5342–5349, 2002.

[19] J. Hofkens, M. Cotlet, T. Vosch, P. Tinnefeld, K. D. Weston, C. Ego, A. Grimsdale, K. Müllen, D. Beljonne, J. L. Brédas, S. Jordens, G. Schweitzer, M. Sauer, and F. D. Schryver, "Revealing competitive Forster-type resonance energy-transfer pathways in single bichromophoric molecules," *Proc. Natl. Acad. Sci. USA*, vol. 100, no. 23, pp. 13146–13151, 2003.

[20] C. G. Hübner, G. Zumofen, A. Renn, A. Herrmann, K. Müllen, and T. Basché, "Photon antibunching and collective effects in the fluorescence of single bichromophoric molecules," *Phys. Rev. Lett.*, vol. 91, no. 9, pp. 093903-01–093903-04, 2003.

[21] D. Nettels, I. Gopich, A. Hoffmann, and B. Schuler, "Ultrafast dynamics of protein collapse from single molecule photon statistics," *Proc. Natl. Acad. Sci. USA*, vol. 104, no. 8, pp. 2655–2660, 2007.

[22] B. Schuler, E. A. Lipman, and W. A. Eaton, "Probing the free-energy surface for protein folding with single-molecule fluorescence spectroscopy," *Nature*, vol. 419, no. 6908, pp. 743–747, 2002.

[23] B. Schuler, E. A. Lipman, P. J. Steinbach, M. Kumke, and W. A. Eaton, "Polyproline and the "spectroscopic ruler" revisited with single molecule fluorescence," *Proc. Natl. Acad. Sci. USA*, vol. 102, pp. 2754–2759, 2005.

[24] W. Kremer, B. Schuler, S. Harrieder, M. Geyer, W. Gronwald, C. Welker, R. Jaenicke, and H. R. Kalbitzer, "Solution NMR structure of the cold-shock protein from the hyperthermophilic bacterium thermotoga maritima," *Eur. J. Biochem.*, vol. 268, no. 9, pp. 2527–2539, 2001.

[25] C. Kurtsiefer, P. Zarda, S. Mayer, and H. Weinfurter, "The breakdown flash of silicon avalanche photodiodes-back door for eavesdropper attacks?" *J. Mod. Opt.*, vol. 48, no. 13, pp. 2039–2047, 2001.

[26] J. Widengren, Ü. Mets, and R. Rigler, "Fluorescence correlation spectroscopy of triplet states in solution—A theoretical and experimental-study," *J. Phys. Chem.*, vol. 99, no. 36, pp. 13368–13379, 1995.

[27] S. Felekyan, R. Kühnemuth, V. Kudryavtsev, C. Sandhagen, W. Becker, and C. A. M. Seidel, "Full correlation from picoseconds to seconds by time-resolved and time-correlated single photon detection," *Rev. Sci. Instrum.*, vol. 76, no. 8, pp. 083104-01–083104-14, 2005.

[28] M. Wahl, H. Rahn, I. Gregor, R. Erdmann, and J. Enderlein, "Dead-time optimized time-correlated photon counting instrument with synchronized, independent timing channels," *Rev. Sci. Instrum.*, vol. 78, no. 3, pp. 033106-1–033106-6, 2007.

Daniel Nettels received the Ph.D. degree in quantum optics and laser spectroscopy from the University of Fribourg, Fribourg, Switzerland, in 2003.

Since 2004, he has been a postdoctoral research fellow with the Department of Biochemistry, University of Zurich, Zurich, Switzerland.

Ben Schuler received the Ph.D. degree in physical biochemistry from the University of Regensburg, Bavaria, Germany.

He was a postdoctoral research fellow in biophysics with the National Institutes of Health, Bethesda, MD. He was the head of an independent research group with the University of Potsdam, Potsdam, Germany, supported by the Emmy Noether Program of the Deutsche Forschungsgemeinschaft. Since 2004, he has been an Assistant Professor with the Department of Biochemistry, University of Zurich, Zurich, Switzerland.